Mixed permutation symmetry quantum phase transitions of critical three-level atom models

A. Mayorgas[1⋆], J. Guerrero[3] and M. Calixto[1,2]

1 Department of Applied Mathematics, University of Granada, Fuentenueva s/n, 18071 Granada, Spain
2 Institute Carlos I of Theoretical and Computational Physics, University of Granada, Fuentenueva s/n, 18071 Granada, Spain
3 Department of Mathematics, University of Jaen, Campus Las Lagunillas s/n, 23071 Jaen, Spain
⋆ albmayrey97@ugr.es

December 22, 2022

34th International Colloquium on Group Theoretical Methods in Physics
Strasbourg, 18-22 July 2022
doi:10.21468/SciPostPhysProc.?

Abstract

We define the concept of Mixed Symmetry Quantum Phase Transition (MSQPT), considering each permutation symmetry sector μ of an identical particles system, as singularities in the properties of the lowest-energy state into each μ when shifting a Hamiltonian control parameter λ. A three-level Lipkin-Meshkov-Glick (LMG) model is chosen to typify our construction. Firstly, we analyze the finite number N of particles case, proving the presence of MSQPT precursors. Then, in the thermodynamic limit $N \to \infty$, we calculate the lowest-energy density inside each sector μ, augmenting the control parameter space by μ, and showing a phase diagram with four different quantum phases.

Contents

1 Introduction

When studying quantum systems of identical particles, e.g. bosons and fermions, permutation symmetry become crucial. There exist more exotic instances such as N identical particles distributed in a set of L levels ($\mathcal{H}_L^{\otimes N}$ as Hilbert space) and a second quantized Hamiltonian describing pair correlations. In particular, the condition of identical atoms allows to use permutation symmetry S_N to decompose $\mathcal{H}_L^{\otimes N}$ into a "Clebsh-Gordan" direct sum of unitary irreducible representations (unirreps or sectors) of U(L). We shall use Young tableaux as a useful graphical method to depict this decomposition.

It is common in the literature the restriction to the totally symmetric unirrep or sector when studying quantum phase transitions (QPTs) of critical quantum systems in the thermodynamic limit $N \to \infty$, like in Refs. [1–3], reducing Hilbert space $\mathcal{H}_L^{\otimes N}$ dimension from L^N to, for example, $N+1$ for $L=2$. This means to make the particles indistinguishable, which is a broadly assumed procedure without any evident physical justification (usually for computational benefit). Therefore, we are devoted to study the role of these often disregarded mixed permutation symmetry sectors in this work. As a paradigmatic case, we will use the Lipkin-Meshkov-Glick (LMG) Hamiltonian for $L=3$ levels (2), where λ will be the control parameter used to detect critical phenomena (QPTs). The case $L=2$ (see [4]) is not considered because all sectors can be reduced to the symmetric one, and the cases $L>3$ provide an extra difficulty when minimizing the energy surface of the Hamiltonian. We address the reader to Ref. [5] for more information.

The organization of this article the following; in the Section 2 we classify the Hamiltonian spectrum and examine the lowest-energy state inside different permutation symmetry sectors for a finite number of particles N. In the Section 3, we find mixed symmetry quantum phase transitions (MSQPTs) in the thermodynamic limit $N \to \infty$. At the end, in Sec. 4, we give the conclusions.

2 The 3-level LMG model. U(L) unirreps and QPT precursors

Models describing pairing correlations are usually described by a Hamiltonian in the second quantization form

$$H_L = \sum_{i=1}^{L}\sum_{\mu=1}^{N} \varepsilon_i c_{i\mu}^{\dagger} c_{i\mu} - \sum_{i,j,k,l=1}^{L}\sum_{\mu,\nu=1}^{N} \lambda_{ij}^{kl} c_{i\mu}^{\dagger} c_{j\mu} c_{k\nu}^{\dagger} c_{l\nu}\,, \tag{1}$$

where $c_{i\mu}$ ($c_{i\mu}^{\dagger}$) destroys (creates) a particle in the μ state of the level i. Precisely, there is a finite number N of identical particles dispersed among L energy levels (N-fold degenerate). Pairs of particles are scattered between the L levels when considering the two-body residual interactions of strength λ, so that the total number of particles remains constant.

In our case, we focus on $L=3$ level systems and apply the following list of restrictions to the Hamiltonian (1): Firstly, we define U(L) "quasispin" collective operators $S_{ij} = \sum_{\mu=1}^{N} c_{i\mu}^{\dagger} c_{j\mu}$. Secondly, we disregard interactions for particles in the same level and consider equal interactions in different levels, i.e. $\lambda_{ij}^{kl} = \frac{\lambda}{N(N-1)}\delta_{ik}\delta_{jl}(1-\delta_{ij})$. Thirdly, we transform the Hamiltonian into an energy density (intensive quantity) by dividing the interaction strength λ by the total particle pairs $N(N-1)$. Fourthly, we place the levels symmetrically about the level $i=2$, $\varepsilon_3 = -\varepsilon_1 = \epsilon/N$ and $\varepsilon_2 = 0$. Eventually, the Hamiltonian turns into the 3-level LMG Hamiltonian,

$$H_3 = \frac{\epsilon}{N}(S_{33} - S_{11}) - \frac{\lambda}{N(N-1)} \sum_{i\neq j=1}^{3} S_{ij}^2\,. \tag{2}$$

It can be regarded as an extension of the paradigmatic $L=2$ levels LMG Hamiltonian used in the shell model [6, 7].

An interesting property of the 3-level LMG Hamiltonian (2) is that the λ-interaction only scatters pairs of particles, and therefore, conserves the parity $\Pi_i = \exp(i\pi S_{ii})$ of the population S_{ii} in each level $i = 1, 2, 3$. Consequently, the parity symmetry is described by the parity group $\mathbb{Z}_2 \times \mathbb{Z}_2 \times \mathbb{Z}_2$ with the constraint $\Pi_1\Pi_2\Pi_3 = (-1)^N$. This symmetry will be spontaneously broken in the thermodynamic limit $N \to \infty$ leading to a highly degenerated ground state. In addition, if we choose basis vectors adapted to irreducible representations of the Lie group $U(3)$, the Hamiltonian matrix (2) will be block diagonal, and hence the procedure presented in the following paragraphs.

We want to focus on the decomposition of the N-fold tensor product Hilbert space $\mathcal{H}_L^{\otimes N}$ of N L-level atoms into U(L) unirreps. In particular, we shall use Young tableaux and Gelfand-Tsetlin (GT) patterns along this article since they are powerful diagrammatic methods (see [8,9] for more details and definitions). The fundamental $L \times L$ representation of U(L) is given by a Young box $\square$, and states of one particle by Weyl patterns/tableaux, $\boxed{1} = |1\rangle$, $\boxed{2} = |2\rangle$, $\boxed{3} = |3\rangle$, ... In the case $L = 3$, we apply the Gram-Schmidt orthonormalization procedure to the columns of a complex triangular matrix T in order to obtain unitary matrices of U(3)

$$T = \begin{pmatrix} 1 & 0 & 0 \\ \alpha & 1 & 0 \\ \beta & \gamma & 1 \end{pmatrix} \xrightarrow{\text{G-S}} V = \begin{pmatrix} \frac{1}{\sqrt{\ell_1}} & \frac{-\bar{\alpha}-\gamma\bar{\beta}}{\sqrt{\ell_1\ell_2}} & \frac{-\bar{\beta}+\bar{\alpha}\bar{\gamma}}{\sqrt{\ell_2}} \\ \frac{\alpha}{\sqrt{\ell_1}} & \frac{1+\beta\bar{\beta}-\alpha\gamma\bar{\beta}}{\sqrt{\ell_1\ell_2}} & \frac{-\bar{\gamma}}{\sqrt{\ell_2}} \\ \frac{\beta}{\sqrt{\ell_1}} & \frac{\gamma-\beta\bar{\alpha}+\gamma\alpha\bar{\alpha}}{\sqrt{\ell_1\ell_2}} & \frac{1}{\sqrt{\ell_2}} \end{pmatrix}, \tag{3}$$

which is parameterized by the complex parameters $\alpha, \beta, \gamma \in \mathbb{C}$, where $\ell_1 = |T^\dagger T|_1 = 1+\alpha\bar{\alpha}+\beta\bar{\beta}$ and $\ell_2 = |T^\dagger T|_2 = 1 + \gamma\bar{\gamma} + (\beta - \alpha\gamma)\left(\bar{\beta} - \bar{\alpha}\bar{\gamma}\right)$. Actually, the addition of the coordinates $u_1, u_2, u_3 \in S^1$ completes the parametrization as $U = V \cdot \mathrm{diag}(u_1, u_2, u_3) \in$U(3).

The L^N-dimensional Hilbert space $\mathcal{H}_L^{\otimes N}$ is represented by the N-fold tensor product representation $\square \otimes \overset{(N)}{\cdots} \otimes \square$. The Hilbert space is reducible into invariant subspaces, which are graphically represented by Young frames of $h_1 + \cdots + h_L = N$ boxes labeled by $h = [h_1, \ldots, h_L]$, where h_i is the number of boxes in a row $i = 1, \ldots, L$, fulfilling $h_1 \geq \cdots \geq h_L$. The unirreps decomposition can be regarded as a generalization of the Clebsch-Gordan decomposition in U(2).

We shall remind that Weyl patterns symbolize the different vectors of a given representation (Young frame). They are in semistandard form when labels (numbers) inside the pattern increase from the right to the left, and strictly increase from the top to the bottom (see [5] for some examples). An important result is that the number of semistandard form Weyl patterns is the dimension of the unirrep. Another useful definition is the weight of a Weyl pattern, which is vector $w = (w_1, \ldots, w_L)$ whose components w_k are the population of level k, with $w_1 + \cdots + w_L = N$. The lexicographical rule states that a state of weight w has lower weight than another with weight w' if the first non-zero coefficient of $w - w'$ is positive. Notably, the highest weight (HW) vector of an unirrep $h = [h_1, h_2, h_3]$ of $U(3)$ is $w = (h_1, h_2, h_3)$.

The semistandard form Weyl patterns are in one-to-one correspondence with Gelfand-Tsetlin (GT) patterns [5, 9], another useful diagrammatic method to express the vectors spanning U(L) unirreps. GT patterns are labeled by vectors $|\mathbb{m}\rangle$, and are useful for obtaining the eigenvalues and matrix elements $\langle \mathbb{m}|S_{ij}|\mathbb{m}'\rangle$ of the collective operators S_{ij} in each unirrep h. This is called the Gelfand-Tsetlin method and is detailed in the reference [5].

From this point on, we shall study the symmetry classification of the LMG U(3) Hamiltonian (2) eigenstates, and some QPT precursors. The free LMG U(3) Hamiltonian is obtained by taking $\lambda = 0$ in (2), $H^{(0)} = \frac{\epsilon}{N}(S_{33} - S_{11})$, $\epsilon > 0$. According to the Lieb-Mattis theorem [10, 11], the lowest-energy eigenstate is the highest weight vector of the fully symmetric unirrep $h = [N, 0, 0]$, which corresponds to arrange all the particles in the level $i = 1$, $|\psi_0\rangle = |\mathbb{m}_{\mathrm{hw}}\rangle = \boxed{1|\cdots|1}$ (N boxes). The excited states have an energy $E_n = \frac{n-N}{N}\epsilon$, $n = 1, \ldots, 2N$, and are highly degenerated, except for E_0 and E_{2N}. For instance, the states $\boxed{1|\cdots|1|2}$ and $\begin{array}{|c|c|c|}\hline 1 & \cdots & 1 \\ \hline 2 \\ \cline{1-1}\end{array}$ have the same energy E_1 (see Ref. [5] for the explicit calculations).

The two-body interactions governed by λ lift the degeneracy of the eigenstates. This is evident in the Figure 1 of the reference [5] when increasing λ, where there are four different unirreps of a LMG U(3) model with $N = 4$ particles. For instance, the lowest energy in the unirrep $h = [3,1,0]$ is below the third lowest energy in $h = [4,0,0]$ for $\lambda < 1$, hence mixed symmetry sectors (such as $h = [3,1,0]$) should not be disregarded in general when studying excited states and their energies.

At this point, it is convenient to define the concept of Mixed Symmetry Quantum Phase Transition (MSQPT) in a nutshell. We want to analyze critical behavior into each Hilbert subspace $\mathcal{H}_h$ corresponding to an unirrep h of $U(3)$, as Hamiltonian evolution does not blend different sectors h. Consequently, we choose the lowest-energy vector $|\psi_0^h\rangle$ inside each $\mathcal{H}_h$, and seek radical changes in its structure when shifting λ in the thermodynamic limit $N \to \infty$. But before doing that, we should consider QPT precursors for finite N, which can anticipate the approximate situation of critical points. One of them is the fidelity [12, 13], measuring how similar (overlap) two states are in the vicinity ($\delta\lambda \ll 1$) of λ, $F_\psi(\lambda, \delta\lambda) = |\langle\psi(\lambda)|\psi(\lambda+\delta\lambda)\rangle|^2$. The fidelity reaches a minimum in the proximity of a critical point $\lambda^{(0)}$, when the state $|\psi(\lambda)\rangle$ suffer a drastic change of its structure. Another precursor, which is less sensitive to the step size $\delta\lambda$, is the susceptibility

$$\chi_\psi(\lambda, \delta\lambda) = 2\frac{1 - F_\psi(\lambda, \delta\lambda)}{(\delta\lambda)^2}, \tag{4}$$

which reaches a maximum in the vicinity of the critical point $\lambda^{(0)}$.

The Figure 1a shows the susceptibility of the ground state (GS) of the LMG U(3) model for a different number of particles N. We have done the calculations numerically, giving a matricial form to the S_{ij} operators using the GT basis $|\mathbb{m}\rangle$ in each unirrep. In particular, thanks to the Lieb-Mattis theorem [10, 11], we know that the GS belongs to the fully symmetric irrep, reducing the computations to $h = [N,0,0]$ in this case. The susceptibility is sharper as N increases, predicting a critical point around $\lambda \simeq 0.55\epsilon$ for the highest $N = 100$ line, which is a precursor of the QPT eventually occurring exactly at $\lambda^{(0)} = 0.5\epsilon$ as we will see in the Section 3.

On the other hand, the Figure 1b displays the susceptibility of the lowest-energy vector inside different mixed symmetry sectors (unirreps h) for a fixed number of particles $N = 30$. Now, the would-be critical points (maximum of the susceptibility) move along the different sectors; they shifted to the right from $h = [30,0,0]$ to $h = [20,10,0]$ (cyan dashed line), and to the left from $h = [20,10,0]$ to $h = [15,15,0]$ (magenta dashed line). Consequently, the figure envisages a quadruple point at the unirrep $h = [2N/3, N/3, 0]$, also called "handgun" sector because of its Young frame shape. The maxima at right in the figure are precursor of another QPT at $\lambda \simeq 1.5\epsilon$, but it is in a different scale and requires a higher N to be properly characterized.

The population densities $\langle\psi_0^h|S_{ii}|\psi_0^h\rangle/N$, of the ground state ψ_0^h inside each sector h, are also good QPT precursors (the reader can find a detailed discussion in Ref. [5]).

3 Thermodynamic limit and MSQPTs

We shall start this section talking about coherent states. They are excellent variational (semiclassical) states, as they reproduce the structure and mean energy of lowest-energy states inside each symmetry sector h at $N \to \infty$. For a detailed explanation, see the reference [4] for the U(2) case. In our case, we follow the Perelomov's construction [14, 15] of the coherent states in a given unirrep h of U(L). Namely, we rotate the HW vector state $|\mathbb{m}_{\rm hw}\rangle$ of an unirrep h by an unitary matrix $U \in$U(3) parameterized as in (3), $|h,U\rangle = K_h(U)|h;\alpha,\beta,\gamma\}$, where $|h;\alpha,\beta,\gamma\} = e^{\beta S_{31}} e^{\alpha S_{21}} e^{\gamma S_{32}} |\mathbb{m}_{\rm hw}\rangle$, and $K_h(U)$ a normalization factor. The coherent state expectation values $s_{ij} = \langle h,U|S_{ij}|h,U\rangle$ of the basic symmetry operators S_{ij} can be easily calculated in the differential representation (see the Appendix A of [5] for a detailed calculation).

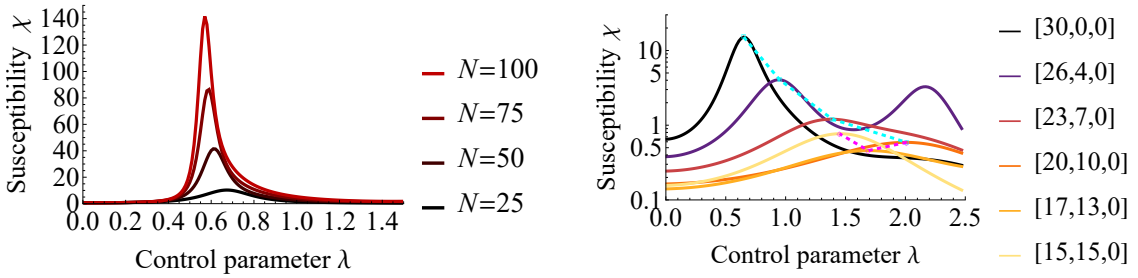

(a) (b)

Figure 1: (a) Susceptibility χ_ψ of the ground state $\psi_0^{h=[N,0,0]}$ of the 3-level LMG Hamiltonian (2) for different values of the control parameter λ and the total number of particles N. It predicts a QPT whose critical point is around $\lambda^{(0)} \simeq 0.55$. (b) Susceptibility $\chi_{\psi_0^h}$ (in logarithmic scale) of the lowest-energy vector ψ_0^h into different sectors h for a fixed number of $N = 30$ atoms. The dashed lines interpolate between the maxima of the susceptibilities, which are precursors of the would-be critical points dividing phase I from phase II (cyan), and phase I from phase IV (magenta) (see later on Figure 2 the different phases). The turn away point, where both dashed lines meet, corresponds to the "hand-gun" unirrep $h = [20, 10, 0]$, where four phases will coincide (see later on Sec. 3). We use ϵ units for λ and a step size $\delta\lambda = 0.01$ in both figures.

Form now on, it is convenient to relabel U(3) unirreps $h = [h_1, h_2, h_3]$ by parameters μ, ν. More explicitly, $h_3 = \nu N$, $h_2 = (1-\mu)(1-\nu)N$, $h_1 = \mu(1-\nu)N$, $\forall\ \nu \in [0, \frac{1}{3}]$, $\mu \in [\frac{1}{2}, \frac{1-2\nu}{1-\nu}]$, so they will become continuous parameters in the thermodynamic limit. Then, we are able to define the energy surface of a Hamiltonian density H into the Hilbert space sector (μ, ν) as $E^U_{\mu,\nu}(\epsilon, \lambda) = \lim_{N\to\infty} \langle h, U|H|h, U\rangle$. That is, the coherent state expectation value of the Hamiltonian density in the thermodynamic limit ($N \to \infty$). In the LMG U(3) case,

$$E^U_{\mu,\nu}(\epsilon, \lambda) = \lim_{N\to\infty} \left(\frac{\epsilon(s_{33} - s_{11})}{N} - \frac{\lambda \sum_{i\neq j=1}^{3} s_{ij}^2}{N(N-1)} \right), \tag{5}$$

which depends on the type of unirrep (μ, ν), the complex coordinates of U (α, β and γ), and the control parameters ϵ and λ. The explicit expression of the matrix elements s_{ij} is given in the Appendix A of [5]. We fix ϵ and measure the energy surface and λ in ϵ units, since $E^U_{\mu,\nu}(\epsilon, \lambda) = \epsilon E^U_{\mu,\nu}(1, \lambda/\epsilon)$. In addition, we benefit from $h = [h_1, h_2, h_3]$ and $h' = [h_1 - h_3, h_2 - h_3, 0]$ being equivalent SU(3) unirreps and obtain the expression $E^U_{\mu,\nu}(\epsilon, \lambda) = (1-3\nu)E^U_{\tilde{\mu},0}(\epsilon, (1-3\nu)\lambda)$, $\tilde{\mu} = \frac{\mu(1-\nu)-\nu}{1-3\nu}$, so we restrict to the study of the parent case $\nu = 0, \mu \in [\frac{1}{2}, 1]$. For $\mu = 1$, we have the totally symmetric representations, with a four-dimensional phase space $\alpha, \beta \in \mathbb{C}$ and an energy surface that is invariant under $\alpha \to -\alpha$, $\beta \to -\beta$, thus preserving the discrete parity symmetry inherited from the Hamiltonian). For $\mu = 1/2$, the representations are linked to rectangular Young tableaux ($h_1 = N/2 = h_2$), and the energy surface $E^U_{\frac{1}{2},0}(\epsilon, \lambda) = \frac{1}{2}E^{(\gamma,\beta')}_{1,0}(\epsilon, \frac{\lambda}{2})$, $\beta' = \beta - \alpha\gamma$, can be obtained from the totally symmetric case. The intermediate values $\mu \in (\frac{1}{2}, 1)$ give a six-dimensional phase space (*flag manifold*) $\alpha, \beta, \gamma \in \mathbb{C}$. The explicit expression of all these energy surfaces can be found in the reference [5].

Henceforward we minimize in the phase space coordinates the energy density of the parent case (take $\nu = 0, \mu \in [\frac{1}{2}, 1]$ in (5)), i.e. we find the minimum energy

$$E^{(0)}_\mu(\epsilon, \lambda) = \min_{U\in U(3)} E^U_{\mu,0}(\epsilon, \lambda), \quad \forall\, \mu \in [\frac{1}{2}, 1]. \tag{6}$$

As we can see in the Figure 2, the representation label μ behaves as an additional control parameter, differentiating four different quantum phases (I, II, III and IV) in the λ-μ plane (color lines). The transitions between phases for $\mu \neq 1$ can be understood as MSQPTs. We can also find the aforementioned quadruple point at $(\lambda, \mu)_q = (3\epsilon/2, 2/3)$, where the four phases coexist. In the Figures 6 and 7 of the main reference [5], we discuss that the MSQPTs are second-order phase transitions as the second derivatives $\partial_{\mu\mu} E_\mu^{(0)}(\epsilon, \lambda)$, $\partial_{\lambda\lambda} E_\mu^{(0)}(\epsilon, \lambda)$, and $\partial_{\mu\lambda} E_\mu^{(0)}(\epsilon, \lambda)$ are discontinuous at critical points.

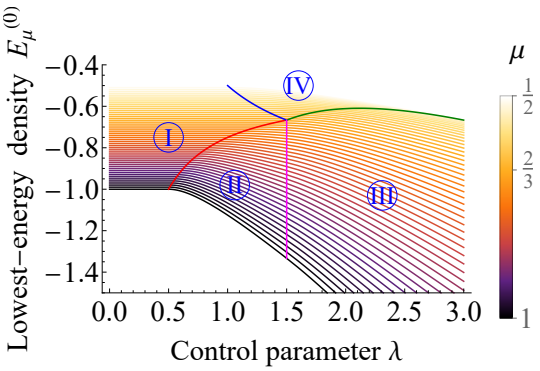

Figure 2: Lowest-energy density $E_\mu^{(0)}(\epsilon, \lambda)$ of the parental case (6) for different values of the control parameter λ and the unirrep continuous parameter μ, varying from $\mu = 1$ (black curve) to $\mu = 1/2$ (light yellow curve), with a step size of $\delta\mu = 0.01$. There are four different quantum phases in the phase diagram, which coincide at a quadruple point $(\lambda, \mu)_q = (3/2, 2/3)$. The phases are separated by curves of critical points in color red, magenta, green, and blue. Both axes are in ϵ units.

The minimization gives many critical points $\alpha_0, \beta_0, \gamma_0$ in the phase space with the same $E_\mu^{(0)}$, so the lowest-energy state for a general μ is highly degenerated. This behavior is easier to show in the fully symmetric case $\mu = 1$ (lowest lines of the Figure 2), where there are three different phases and two second-order QPTs at $\lambda^{(0)}_{\mathrm{I}\leftrightarrow\mathrm{II}} = \epsilon/2$ and $\lambda^{(0)}_{\mathrm{II}\leftrightarrow\mathrm{III}} = 3\epsilon/2$. The critical values of α and β which make the energy surface minimum are real numbers which have the properties $\alpha_0^{\pm}(\epsilon, \lambda) = 0$ $\forall 0 \leq \lambda \leq \frac{\epsilon}{2}$, and $\beta_0^{\pm}(\epsilon, \lambda) = 0$ $\forall\, 0 \leq \lambda \leq \frac{3\epsilon}{2}$ (check the reference [5] for an explicit expression of the minimum energy surface and the critical points). Therefore, there is a single minimum in phase I, $0 \leq \lambda/\epsilon \leq 1/2$, located at $\alpha = \beta = 0$; a double minimum in phase II, $1/2 \leq \lambda/\epsilon \leq 3/2$,, with $\beta = 0$; and a quadruple minimum in phase III, $\lambda/\epsilon \geq 3/2$. This degenerated minima effect is due to the spontaneous breakdown of the discrete parity symmetry of the Hamiltonian, as in the limit $N \to \infty$, the four coherent states $|\alpha_0^{\pm}, \beta_0^{\pm}\rangle$ reach the same minimum energy $E_1^{(0)}$ (minimization of the symmetric case $\mu = 1$, $\nu = 0$ in (5)). The parity restoration of the GS is discussed in the references [5, 16, 17].

4 Conclusion

QPTs research in many-body systems usually presuppose the particle indistinguishability, restricting the scope to the fully symmetric representation ($\mu = 1$), which is often not a general procedure. That is why we have defined MSQPTs as QPTs of the lowest-energy state in a particular symmetry sector μ. As a test model, we have chosen an extension of the ubiquitous LMG model to $L = 3$ levels.

Firstly, we have done numerical calculations for a finite number of particles N to obtain QPT precursors, such as the susceptibility, which anticipate the QPT in the thermodynamic limit

$N \to \infty$. In general, the precursors give a better approximation to the critical points when increasing N.

Secondly, using coherent (semiclassical) states, we have considered the thermodynamic limit $N \to \infty$ and minimized the energy surface in different unirreps. The critical points $\lambda^{(0)}$, where the MSQPTs occur, turn out to depend on the representation index μ. Therefore, we have extended the phase diagram in an extended control parameter space (λ, μ). In addition, there are evidences of a quadruple point where four different phases coincide at $\mu = 2/3$. We have also discussed that the lowest-energy state for general representation μ is degenerated, because of the spontaneous breakdown of the discrete parity symmetry of the Hamiltonian in the limit $N \to \infty$.

To conclude, we propose for further research the possible overlap between MSQPT and ESQPT [18], and the exploitation of permutation symmetry in the realm of quantum technologies [19].

Acknowledgements

We thank the organizers of the 34th edition of the ICGTMP for their hospitality and the preparation of the congress. We are also glad to have shared the interesting discussions with J.P. Gazeau, M.A. del Olmo, M.A. Lledó, P. Van Isacker, D. Schuch, and F.J. Herranz during the sessions. We thank O. Castaños and E. Perez-Romero for their collaboration in this work.

Funding information We thank the support of the Spanish MICINN through the project PGC2018-097831-B-I00 and Junta de Andalucía through the projects UHU-1262561, FQM-381 and FEDER/UJA-1381026. AM thanks the Spanish MIU for the FPU19/06376 predoctoral fellowship.

References

[1] S. Gnutzmann and M. Kuś, *Coherent states and the classical limit on irreducible su3 representations*, Journal of Physics A: Mathematical and General **31**, 9871 (1999), doi:10.1088/0305-4470/31/49/011.

[2] S. Gnutzmann, F. Haake and M. Kuś, *Quantum chaos of su3 observables*, Journal of Physics A: Mathematical and General **33**, 143 (1999), doi:10.1088/0305-4470/33/1/309.

[3] D. C. Meredith, S. E. Koonin and M. R. Zirnbauer, *Quantum chaos in a schematic shell model*, Phys. Rev. A **37**, 3499–3513 (1988), doi:10.1103/PhysRevA.37.3499.

[4] O. Castaños, R. López-Peña, J. G. Hirsch and E. López-Moreno, *Classical and quantum phase transitions in the Lipkin-Meshkov-Glick model*, Phys. Rev. B **74**, 104118 (2006), doi:10.1103/PhysRevB.74.104118.

[5] M. Calixto, A. Mayorgas and J. Guerrero, *Role of mixed permutation symmetry sectors in the thermodynamic limit of critical three-level Lipkin-Meshkov-Glick atom models*, Phys. Rev. E **103**, 012116 (2021), doi:10.1103/PhysRevE.103.012116.

[6] H. J. Lipkin, N. Meshkov and A. J. Glick, *Validity of many-body approximation methods for a solvable model. (i). exact solutions and perturbation theory*, Nuclear Physics **62**(2), 188–198 (1965), doi:10.1016/0029-5582(65)90862-X.

[7] H. J. Lipkin, N. Meshkov and A. J. Glick, *Validity of many-body approximation methods for a solvable model: (iii). diagram summations*, Nuclear Physics **62**(2), 211–224 (1965), doi:10.1016/0029-5582(65)90864-3.

[8] W. Greiner and B. Müller, *Quantum Mechanics. Symmetries*, Springer, doi:https://doi.org/10.1007/978-3-642-57976-9 (1994).

[9] L. C. Biedenharn and J. Louck, *Angular Momentum in Quantum Physics: Theory and Application*, Encyclopedia of Mathematics and its Applications. Cambridge University Press, doi:10.1017/CBO9780511759888 (1984).

[10] E. Lieb and D. Mattis, *Theory of ferromagnetism and the ordering of electronic energy levels*, Phys. Rev. **125**, 164–172 (1962), doi:10.1103/PhysRev.125.164.

[11] M. Calixto, A. Mayorgas and J. Guerrero, *Hilbert space structure of the low energy sector of u(n) quantum hall ferromagnets and their classical limit*, Symmetry **14**(5) (2022), doi:10.3390/sym14050872.

[12] S.-J. Gu, *Fidelity approach to quantum phase transitions*, International Journal of Modern Physics B **24**(23), 4371–4458 (2010), doi:10.1142/S0217979210056335.

[13] P. Zanardi, P. Giorda and M. Cozzini, *Information-theoretic differential geometry of quantum phase transitions*, Phys. Rev. Lett. **99**, 100603 (2007), doi:10.1103/PhysRevLett.99.100603.

[14] A. Perelomov, *Generalized Coherent States and Their Applications*, Springer-Verlag Berlin Heidelberg, doi:10.1007/978-3-642-61629-7 (1986).

[15] J. Gazeau, *Coherent States in Quantum Physics*, John Wiley & Sons, Ltd, ISBN 9783527628285, doi:10.1002/9783527628285 (2009).

[16] M. Calixto, A. Mayorgas and J. Guerrero, *Entanglement and U(D)-spin squeezing in symmetric multi-qudit systems and applications to quantum phase transitions in Lipkin–Meshkov–Glick D-level atom models*, Quantum Information Processing **20**(9), 304 (2021), doi:10.1007/s11128-021-03218-6.

[17] A. Guerrero, J. Mayorgas and M. Calixto, *Information diagrams in the study of entanglement in symmetric multi-qudit systems and applications to quantum phase transitions in lipkin–meshkov–glick d-level atom models*, Quant. Inf. Process. **21**, 223 (2022), doi:10.1007/s11128-022-03524-7.

[18] M. A. Caprio, P. Cejnar and F. Iachello, *Excited state quantum phase transitions in many-body systems*, Annals of Physics **323**(5), 1106–1135 (2008), doi:10.1016/j.aop.2007.06.011.

[19] N. M. Myers and S. Deffner, *Bosons outperform fermions: The thermodynamic advantage of symmetry*, Phys. Rev. E **101**, 012110 (2020), doi:10.1103/PhysRevE.101.012110.